Mem. S.A.It. Suppl. Vol. 18, 169

Memorie della
Supplementi

Long-lived double-barred galaxies in N-body simulations

J. Shen[1] and V. P. Debattista[2]

[1] Department of Astronomy, University of Texas, Austin, TX, USA
e-mail: shen@astro.as.utexas.edu
[2] Centre for Astrophysics, University of Central Lancashire, Preston, UK

Abstract. Many barred galaxies harbor small-scale secondary bars in the center. The evolution of such double-barred galaxies is still not well understood, partly because of a lack of realistic N-body models with which to study them. Here we report the generation of such systems in the presence of rotating pseudobulges. We demonstrate with high mass and force resolution collisionless N-body simulations that long-lived secondary bars can form spontaneously without requiring gas, contrary to previous claims. We find that secondary bars rotate faster than primary ones. The rotation is not rigid: the secondary bars pulsate, with their amplitude and pattern speed oscillating as they rotate through the primary bars. This self-consistent study supports previous work based on orbital analysis in the potential of two rigidly rotating bars. We also characterize the density and kinematics of the N-body simulations of the double-barred galaxies, compare with observations to achieve a better understanding of such galaxies. The pulsating nature of secondary bars may have important implications for understanding the central region of double-barred galaxies.

1. Introduction

Recent imaging surveys have revealed the frequent existence of nuclear bars in a large number of barred galaxies, e.g., Erwin & Sparke (2002) found that double-barred galaxies are surprisingly common: at least one quarter of their sample of 38 early-type optically-barred galaxies harbor small-scale secondary bars. They found that a typical secondary bar is about 12% the size of its primary counterpart. The facts that inner bars are also seen in near-infrared (e.g., Mulchaey et al. 1997; Laine et al. 2002), and they are often found in gas-poor S0s indicate that most of them are stellar structures. Results from these surveys also show inner bars are at a random angle relative to the primary bars, implying that they are probably dynamically independent structures. Shlosman et al. (1989) invoked multiple nested bars to channel gas inflow into galactic centers to feed AGN, in a similar fashion as the primary bar drives gas inward. However, recent work suggests that this mechanism may not be as efficient as originally hoped (e.g., Maciejewski et al. 2002).

Simulations offer the best way to understand double barred systems. However, the decoupled nuclear bars that formed in early simulations did not last long. For example, the most long-lived nuclear bar in Friedli & Martinet (1993) lasted for less than two turns of the primary bar, corresponding to about 0.4 Gyr, which is far too short to explain the observed

Send offprint requests to: Juntai Shen abundance of nested bars. Furthermore, their models usually require substantial amounts of gas to form and maintain these nuclear bars. Heller et al. (2007a,b) reported that nested bars form in a quasi-cosmological setting, but the amplitudes of the bars also seem to weaken rapidly after most of gas has formed stars (Heller et al. 2007a). Petitpas & Wilson (2004) found that 4 out of 10 double-barred galaxies contain very little molecular gas in the nuclear region. These clues suggest that large amounts of molecular gas may not be necessary to maintain central nuclear bars.

On the side of orbital studies, Maciejewski & Sparke (1997, 2000) discovered a family of loop orbits that may form building blocks of long-lived nuclear stellar bars (see also Maciejewski & Athanassoula 2007). Their studies are very important for understanding double barred galaxies, but their models are not fully self-consistent, since nested bars in general cannot rotate rigidly through each other (Louis & Gerhard 1988). So fully self-consistent N-body simulations are still needed to check if their main results still hold when the non-rigid nature of the bars is taken into account.

Here we demonstrate that long-lived secondary bars can form in purely collisionless N-body simulations, when a rotating pseudobulge is introduced in the model (see also Debattista & Shen 2007; Shen & Debattista 2009). The nuclear bars in our work are distinctly bars, and do not have a spiral shape. We show that the behavior of our models are in good agreement with the loop orbit predictions of Maciejewski & Sparke (2000). We also analyze the photometrical and kinematical properties of high resolution models. Our theoretical results can also be compared to the observed 2D kinematics of some double-barred galaxies, to achieve a better understanding of the dynamics of the secondary bars.

2. Model setup

Our high-resolution simulation consists of a live disk and bulge component. We do not include a halo component for simplicity, also because secondary bars are very small-scale phenomena in galactic centers where visible matter is dominant. The initial disk has the exponential surface density profile and Toomre's $Q \sim 2.0$. The bulge was generated using the method of Prendergast & Tomer (1970) as described in Debattista & Sellwood (2000), where a distribution function is integrated iteratively in the global potential, until convergence. The bulge has the mass of $M_{\rm b} = 0.2M_{\rm d}$. The bulge set up this way is un-rotating, we then give the rotation of the bulge by simply reversing the negative azimuthal velocities of all bulge particles into the same positive values. We have checked that systems set up this way are in very good virial equilibrium.

3. Results

Fig. 1 shows the projected double-barred model (at $t = 405$ when the two bars are nearly perpendicular) with an ordinary orientation: the system is inclined at $i = 45°$ with the line of nodes (LON) of $\psi_{\rm nuc} = 45°$ relative to the secondary bar major axis. The surface density image and contours resemble many observed double-barred systems, such as NGC 2950, even though we did not deliberately set out to match it.

Fig. 2 shows radial variations of $m = 2$ Fourier amplitude and phase for run D at $t = 400$. Fig. 3 shows the ellipticity and position angle (PA) profiles of ellipses fitted with IRAF for the same data as in Fig. 2 (we use log scale for radius to be consistent with what observers usually adopt). There are four popular methods for determining the semi-major axis $a_{\rm B}$ of a bar, as summarized by O'Neill & Dubinski (2003) and Erwin (2005). For convenience, we denote the primary bar as B1 and the secondary bar as B2:

(1) the bar end is measured by extrapolating half-way down the slope on the $m = 2$ amplitude plot (Fig 2a). We find $a_{\rm B1} \sim 2.3$, $a_{\rm B2} \sim 0.4$, the B2/B1 bar length ratio is about ~ 0.17.
(2) the bar end is measured when $m = 2$ phase deviates from a constant by 10° (Fig 2b). We find $a_{\rm B1} \sim 2.1$, $a_{\rm B2} \sim 0.4$, the B2/B1 bar length ratio is about ~ 0.19.

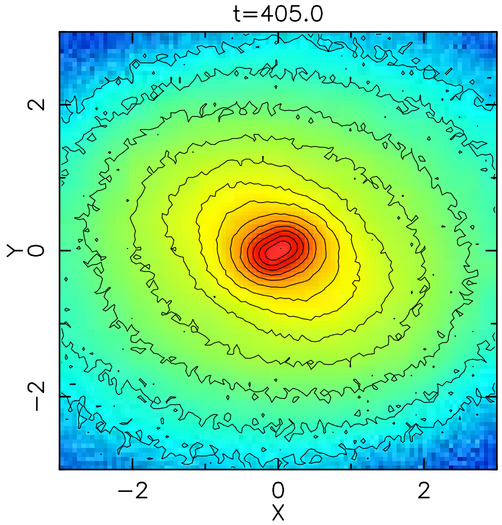

Fig. 1. The double-barred model at $t = 405$ projected to $i = 45°$ and $\psi_{\rm nuc} = 45°$ with all particles shown. The model bears a passing resemblance to NGC 2950.

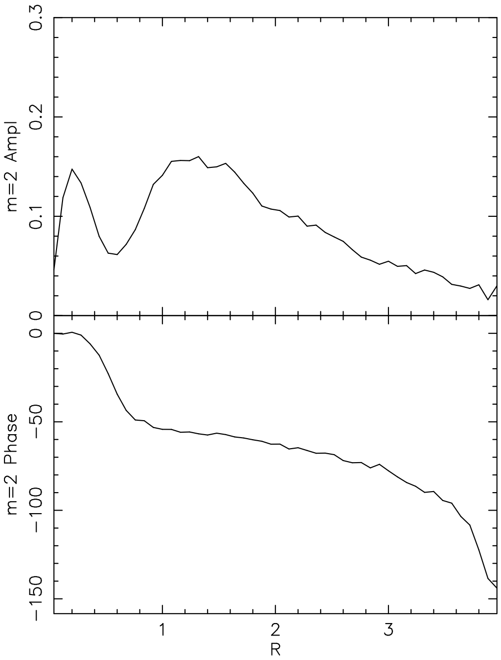

Fig. 2. The radial variations of the m =2 Fourier amplitude and phase of all particles for Run D at t = 400.

(3) the bar end is measured at the peak of the fitted ellipticity profiles (e.g., Marinova & Jogee 2007; Menéndez-Delmestre et al. 2007), which is shown in Fig 3a. We find $a_{\rm B1} \sim 1.7$, $a_{\rm B2} \sim 0.2$, the B2/B1 bar length ratio is about ~ 0.12.

(4) the bar end is measured when the PA of fitted ellipses deviates from a constant by 10° (Fig 3b). We find $a_{\rm B1} \sim 2.3$, $a_{\rm B2} \sim 0.4$, the B2/B1 bar length ratio is about ~ 0.17.

Method 1, 2 and 4 yield consistent values of the bar lengths and length ratios. We found that method 3 tends to give a lower value of bar lengths than the other three methods, as shown in O'Neill & Dubinski (2003). Although these methods have some uncertainties in measuring the bar lengths, the length ratio of the two bars is in the range of 0.12 to 0.19 (in particular method 1, 2, and 4 give a consistent narrow range of 0.17 to 0.19). This result is in good agreement with the typical observed length ratio of local S2B systems (median ratio ~ 0.12, see Erwin & Sparke 2002; Erwin 2004; Lisker et al. 2006). Note that we expect that the length of the secondary cannot be too large, otherwise the gravitational torque from the primary bar will inevitably twist the secondary into alignment if they rotate at different pattern speeds.

Fig. 4 shows the behavior of the azimuthally averaged Ω, $\Omega \pm \kappa/2$, and the location of the Lindblad resonances of the bars at around $t = 400$. As shown in Debattista & Shen (2007), the pattern speeds of the bars, especially that of the secondary, vary as they rotate through each other: the secondary bar rotates slower than average when the two bars are perpendicular, and faster when the bars are parallel. The patten speed bands shown in Fig. 4 reflect such variations. Clearly the pattern speed of the secondary bar oscillates much more than that of the primary. The primary bar extends roughly to its CR radius ($\sim$ 2.5), consistent with the general expectation and is therefore considered a fast bar (e.g., Corsini et al. 2003; Debattista & Williams 2004). The secondary bar rotates faster than the primary bar. However, the secondary bar is much shorter than its shortest $R_{\rm CR}$. In addition, even if the variation of the pattern speed

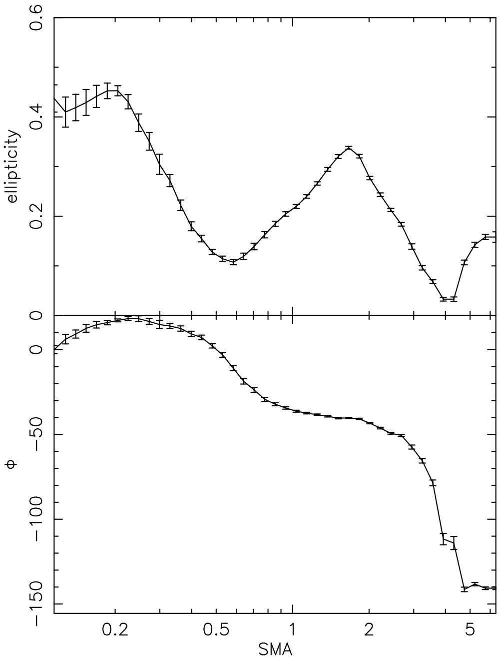

Fig. 3. Ellipticity and position angle as a function of semi-major axis of IRAF-fitted ellipses for Run D at $t = 400$.

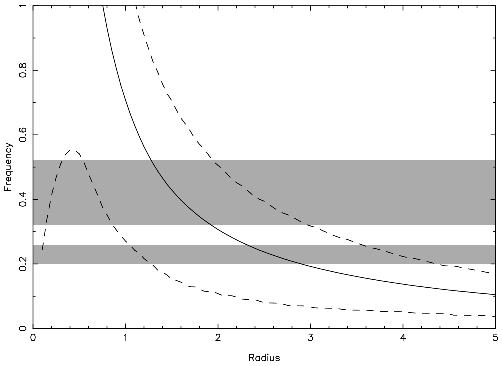

Fig. 4. Frequencies as a function of radius at around $t = 400$ for run D, calculated based on the azimuthally averaged gravitational attraction. The full-drawn line shows the curve of the circular angular frequency Ω and the dashed curves mark $\Omega \pm \kappa/2$, where κ is the epicyclic frequency. The two shaded bands show the oscillational ranges of the bar pattern speeds (the upper band is for the secondary bar and the lower one is for the primary).

is taken into account, the $R_{\rm CR}$ of the secondary is not very close to the $R_{\rm ILR}$ of the primary, if we use the same naive definition of $R_{\rm ILR}$ as in Pfenniger & Norman (1990)[1]. This is inconsistent with the CR-ILR coupling proposed to be a requirement for making secondary bars (e.g., Pfenniger & Norman 1990; Friedli & Martinet 1993).

We also analyzed the line-of-sight velocity distribution (LOSVD) by measuring the mean velocity $\overline{v}$ and velocity dispersion σ. Departures from a Gaussian distribution are parametrized by Gauss-Hermite moments (Gerhard 1993; van der Marel & Franx 1993; Bender et al. 1994). The second order term in such an expansion is related to the dispersion. h_3 measures deviations that are asymmetric about the mean, while h_4 measures the lowest order symmetric deviations from Gaussian (negative for a 'flat-top' distribution, and positive for a more peaked one).

The most striking feature in Fig. 5 is that the twist of the kinematic minor axis (i.e., $v_{\rm los} = 0$) in the secondary bar region is weak (see the mean velocity maps in Fig. 5a, 5b). The kinematic minor axis is almost perpendicular to the inclination axis, although there is a small but noticeable twisted pinch near the kinematic minor axis in the nuclear region. The weak central twist is mainly due to the relatively large velocity dispersion, especially in the central region (likewise at $t = 20$ when only the small nuclear bar exists, the stellar twist is stronger than at $t = 405$, but still quite small compared to the expected twist in gaseous kinematics). On the other hand, the twist of the kinematic *major* axis is more prominent in the central region. Moiseev et al. (2004) found the stellar kinematic minor axis hardly twists from the PA of the disk in their sample with the most reliable kinematics, leading them to question whether nuclear photometric isophotal twists represent *bona fide* dynamically decoupled secondary bars. We demonstrate that an authentic decoupled secondary bar may in-

[1] A cautionary note is that the $R_{\rm ILR}$ read naively from Fig. 4 serves just as a visual guide, because the $R_{\rm ILR}$ determined this way is reliable only for weak bars, and is questionable for our strong bars (e.g., van Albada & Sanders 1982).

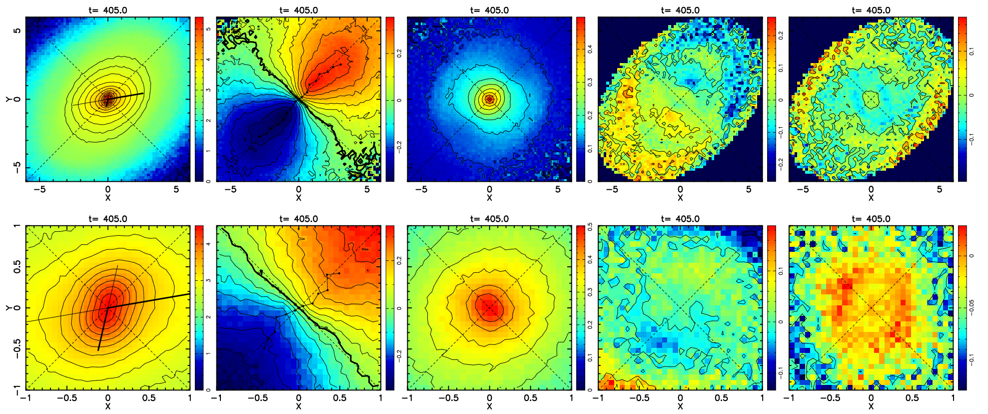

Fig. 5. Photometrical and kinematic maps of our double-barred model. For each row from left to right are the projected surface density, mean velocities, velocity dispersion, h_3, and h_4 maps. (a): Row 1, the double-barred model at $t = 405$ inclined at 45° with the LON of 45° relative to the primary bar major axis; (b): Row 2, close-up view of (a). One of the dashed lines represents the line of nodes (45°), while the other dashed is the anti-LOS (135°).

deed produce a very weak twist of the kinematic minor axis in the stellar velocity field. So a central stellar velocity map without a strong twist as in Moiseev et al. (2004) does not necessarily exclude the existence of a decoupled nuclear bar.

4. Conclusions

We have analyzed the photometrical and kinematical properties of our high resolution models, and contrasted them when with or without a secondary bar. This study also compared the simulated secondary bars with observations.

In general the shape of secondary bars in our models is reasonable compared to observed ones. The length ratio of two bars, determined by various methods, is in the range of 0.12 to 0.19, in good agreement with Erwin & Sparke (2002, 2003). The primary extends roughly to its corotation radius, and therefore fits the definition of a fast bar (see for example Aguerri et al. 2003). Although the secondary bar rotates more rapidly than the primary, its semi-major axis is much shorter than its corotation radius, even if we take the oscillation of the bar patterns speeds into account. We did not find evidence of CR-ILR coupling (e.g., Pfenniger & Norman 1990; Friedli & Martinet 1993) in our models.

We find that the central twist of kinematic axes is quite weak even if a secondary bar is present, due to the relatively large velocity dispersion of stars in the central region. This is consistent with the 2D stellar kinematics of secondary bars studied in Moiseev et al. (2004). We do not find a σ (velocity dispersion) drop for our secondary bar model. It is more likely that σ-drops are just the signature of newly-formed stars, and it is not necessarily a unique feature of double-barred systems.

The general agreement between our simulations and observations of double barred galaxies gives us confidence that the simulations are capturing the same dynamics as in nature. This is especially remarkable because secondary bars are not merely scaled down versions of primary bars, but have distinctly different kinematic properties. In the absence of self-consistent simulations, earlier orbit-based models could not directly confront the challenge from observations which found such differences. This demonstrates the advantage of finally being able to simulate stellar double-barred galaxies, which had been puzzling for so long.

Acknowledgements. JS acknowledges support from a Harlan J. Smith fellowship of McDonald Observatory of UT Austin. VPD was supported by a Brooks Prize Fellowship at the University of Washington and received partial support from NSF ITR grant PHY-0205413.

References

Aguerri, J. A. L., Debattista, V. P., & Corsini, E. M. 2003, MNRAS, 338, 465
Bender, R., Saglia, R. P., & Gerhard, O. E. 1994, MNRAS, 269, 785
Corsini, E. M., Debattista, V. P., & Aguerri, J. A. L. 2003, ApJ, 599, L29
Debattista, V. P., & Sellwood, J. A. 2000, ApJ, 543, 704
Debattista, V. P., & Shen, J. 2007, ApJ, 654, L127
Debattista, V. P., & Williams, T. B. 2004, ApJ, 605, 714
Erwin, P. 2004, A&A, 415, 941
Erwin, P. 2005, MNRAS, 364, 283
Erwin, P., & Sparke, L. S. 2002, AJ, 124, 65
Erwin, P., & Sparke, L. S. 2003, ApJS, 146, 299
Friedli, D., & Martinet, L. 1993, A&A, 277, 27
Gerhard, O. E. 1993, MNRAS, 265, 213
Heller, C. H., Shlosman, I., & Athanassoula, E. 2007a, ApJ, 657, L65
Heller, C. H., Shlosman, I., & Athanassoula, E. 2007b, ApJ, 671, 226
Laine, S., Shlosman, I., Knapen, J. H., & Peletier, R. F. 2002, ApJ, 567, 97
Lisker, T., Debattista, V. P., Ferreras, I., & Erwin, P. 2006, MNRAS, 370, 477
Louis, P. D., & Gerhard, O. E. 1988, MNRAS, 233, 337
Maciejewski, W., & Athanassoula, E. 2007, MNRAS, 380, 999
Maciejewski, W., & Sparke, L. S. 1997, ApJ, 484, L117
Maciejewski, W., & Sparke, L. S. 2000, MNRAS, 313, 745
Maciejewski, W., Teuben, P. J., Sparke, L. S., & Stone, J. M. 2002, MNRAS, 329, 502
Marinova, I., & Jogee, S. 2007, ApJ, 659, 1176
Menéndez-Delmestre, K., Sheth, K., Schinnerer, E., Jarrett, T. H., & Scoville, N. Z. 2007, ApJ, 657, 790
Moiseev, A. V., Valdés, J. R., & Chavushyan, V. H. 2004, A&A, 421, 433
Mulchaey, J. S., Regan, M. W., & Kundu, A. 1997, ApJS, 110, 299
O'Neill, J. K., & Dubinski, J. 2003, MNRAS, 346, 251
Petitpas, G. R., & Wilson, C. D. 2004, ApJ, 603, 495
Pfenniger, D., & Norman, C. 1990, ApJ, 363, 391
Prendergast, K. H., & Tomer, E. 1970, AJ, 75, 674
Shen, J., & Debattista, V. P. 2009, ApJ, 690, 758
Shlosman, I., Frank, J., & Begelman, M. C. 1989, Nature, 338, 45
van Albada, T. S., & Sanders, R. H. 1982, MNRAS, 201, 303
van der Marel, R. P., & Franx, M. 1993, ApJ, 407, 525